PERGAMON

International Journal of Heat and Mass Transfer 45 (2002) 1653–1660

International Journal of HEAT and MASS TRANSFER

www.elsevier.com/locate/ijhmt

Modeling of gaseous radiant exchange with the smooth (reordered) band model

A. Runstedtler [a,*], K.G.T. Hollands [b]

[a] Department of Natural Resources Canada, CANMET Energy Technology Centre, Ottawa, Ont., Canada K1A 1M1
[b] Department of Mechanical Engineering, University of Waterloo, Waterloo, Ont., Canada

Received 3 April 2001; received in revised form 15 August 2001

Abstract

The smooth band model (also called the reordered band model) shows promise of providing the foundation for a radiant analysis method for enclosures containing participating gases. Existing models for the smooth absorption coefficient distribution, however, are not totally satisfactory. This paper presents a new model for the smooth absorption coefficient that addresses the problems with the current models. The new model is exercised on some benchmark calculations of total gas emissivity to test its accuracy. Also, a demonstration problem involving a spherical enclosure with reflective walls is solved to illustrate the utility of the smooth band model, as well as the ease of calculation.

1. Introduction

Radiant analysis for situations where there is a participating gas like CO_2 and H_2O is important in boilers, furnaces, and in the atmosphere, as well as in other engineering situations. The gaseous participation is restricted to certain bands in the infra-red spectrum, called vibration–rotation bands. Characterizing the absorption coefficient in accordance with its exact fine structure inside these bands has proven impractical for the design calculations. The highly complex, rather erratic nature of the absorption spectrum means that even if this fine structure were available over the full temperature range of interest – often it is not – the computational effort is too great for realistic simulations in a design framework. Consequently there have been a number of simpler, approximate methods advanced, such as the correlated-k method, the weighted sum of gray gases method, and the reordered band method. Work on the last of these, the reordered band method, indicates that replacing the actual erratic distribution of a single vibration–rotation band with a smooth, reordered absorption coefficient distribution, $a_\eta(\eta)$, shows promise of providing the foundation for an efficient and general-purpose method that is accurate enough for engineering purposes [1–3]. The "smoothness" is obtained by reordering all the small (infinitesimal) wave number intervals inside a single band in such a way that the reordered distribution either decreases or increases monotonically with wave number, depending on which side of the band center the wave number lies. The smooth band can then be analyzed by marching through the complete wavelength spectrum obtained after re-arranging. Since one can use relatively large wavelength intervals in this marching process, the computational effort is much reduced, and may be realistic for the design context. For reasons that will be made clear, the existing models for the reordered, smooth band function, $a_\eta(\eta)$, are not totally satisfactory. This paper presents a new model for $a_\eta(\eta)$ and exercises it on some benchmark calculations of total gas emissivity and a demonstration problem involving a spherical enclosure.

The smooth reordered band information can also provide basic information for the k-distribution method, the main distinction between these two methods being that in the reordered band approach, the integration is carried out over wave number directly, whereas in the k-distribution method, there is a transformation from wave number to absorption coefficient (sometimes called k), and then the integration is carried out over the

* Corresponding author. Tel.: +1-613-996-7932; fax: +1-613-992-9335.
E-mail address: arunsted@nrcan.gc.ca (A. Runstedtler).

0017-9310/02/$ - see front matter
PII: S0017-9310(01)00268-X

Nomenclature

$A_l(s)$	effective bandwidth (cm^{-1}) of band l for path length s
A^*	dimensionless effective bandwidth; $A^* = A_l(s)/\omega$
a_η	Absorption coefficient (m^{-1})
a^*_η	dimensionless absorption coefficient; $a^*_\eta = \omega a_\eta/(\alpha\rho_a)$
B	coefficient for computing a^*_η in the new absorption coefficient model; see Eqs. (4) and (7)
$b_{i,j}$	coefficients for the new absorption coefficient model; see Eq. (9) and Table 1
$c_{j,k}$	coefficients for the new absorption coefficient model; see Eq. (4) and Table 2
e	a constant ($e = 2.718\ldots$)
$e_{b\eta}(T_g)$	spectral hemispherical emissive power (W/m^2 μm) of a blackbody at temperature T_g
$f(t)$	a function obtained by performing the operation $L^{-1}\{A'_l(s)\}$; see Eq. (1)
j	refers to a specific value of $\log_{10}\beta$; see Eq. (9) and Table 1
L	path length (m) or (cm)
m	the interval in which a given value of β lies; see Eq. (6)
p	a counting variable
P_{CO_2}	partial pressure of CO_2 (atm) or (bar)
P_{total}	total pressure of the gas mixture (atm)
q_w	net *total* radiant heat flux into the wall (W/m^2)
$q_{w\eta}$	net *spectral* radiant heat flux into the wall (W/m^2 μm); see Eq. (11)
R	radius of a sphere (m)
s	path length (m)
T_g	gas temperature (°C) or (K)
T_w	wall temperature (K)
t	a dummy variable; see Eq. (1)

Greek symbols

α	band strength parameter (m^{-1} $cm^{-1}/(g/m^3)$)
β	line overlap parameter (dimensionless); equal to π times the ratio of line width to average line spacing
χ	line overlap parameter (dimensionless) to input to the new absorption coefficient model; see Eq. (5)
δ	the Kronecker delta
$\varepsilon(L)$	total emissivity (dimensionless) of a gas for path length L; see Eq. (10)
ε_w	emissivity (dimensionless) of the wall
η	wave number (cm^{-1})
η_c	wave number (cm^{-1}) at the band centre
η^*	dimensionless wave number; $\eta^* = \lvert\eta - \eta_c\rvert/(\omega/2)$
θ	a function of dimensionless wave number; see Eq. (8)
ρ_a	partial density (g/m^3) of participating gas component 'a'
σ	Stephan–Boltzmann constant; $\sigma = 5.67 \times 10^{-8}$ $W/(m^2\ K^4)$
τ	dimensionless path length; $\tau = \alpha\rho_a s/\omega$
$\overline{\tau}_\eta$	average spectral transmissivity (dimensionless) for the spherical enclosure with reflecting walls; see Eq. (12)
ω	a measure of the wide bandwidth (cm^{-1})

Subscripts

a	refers to participating gas component 'a'
b	refers to a blackbody
CO_2	refers to carbon dioxide gas
c	refers to the band centre
g	refers to the gas
i	refers to the ith coefficient in the new smooth absorption coefficient model; see Eq. (9) and Table 1
j	refers to a specific value of $\log_{10}\beta$; see Eq. (9) and Table 1
k	refers to the kth value of a^*_η; see Eqs. (4) and (9)
l	refers to the lth wide band
p	a counting subscript
total	refers to the entire gas mixture
w	refers to the wall
η	refers to wave number

absorption coefficient rather than wave number itself. The smooth reordered band information also has application to the weighted sum of gray gases method.

2. Background

As was shown by Lee et al. [1], the smooth absorption coefficient distribution can be inferred from existing knowledge of the well-studied effective bandwidth, $A_l(s)$, and its dependence on the path length, s. In particular, they showed that the reordered band can be obtained through finding the inverse Laplace transform $f(t)$ of the derivative, $A'_l(s)$, of $A_l(s)$ and then performing an integral: thus

$$\eta(a_\eta) = \frac{1}{2}\int_{a_\eta}^{\infty}\frac{f(t)}{t}\,\mathrm{d}t = \frac{1}{2}\int_{a_\eta}^{\infty}\frac{L^{-1}\{A'_l(s)\}}{t}\,\mathrm{d}t. \qquad (1)$$

This process defined by Eq. (1) can be done "once for all" and the resulting $\eta(a_\eta)$ function can be presented in a readily useable form [1].

There are certain parameters in the relations for $A_l(s)$ and $a_\eta(\eta)$, namely the band properties, which are the band center wave number η_c, the line overlap parameter β (equal to π times the ratio of line width to average line spacing), the parameter ω (a measure of the band's width), and the group $\alpha\rho_a/\omega$, where α is the band strength parameter, and ρ_a is the partial pressure of the "active" constituent of the gas mixture, i.e., the constituent responsible for the band's presence in the spectrum. The functional relation $a_\eta(\eta)$ can be dedimensionalized. The dimensionless wave number is $\eta^* = |\eta - \eta_c|/(\omega/2)$ and the dimensionless absorption coefficient is $a^*_\eta = \omega a_\eta/(\alpha\rho_a)$. The relation $a_\eta(\eta)$ is then expressed by

$$a^*_\eta = a^*_\eta(\eta^*, \beta). \tag{2}$$

It is noted that the procedure given by Eq. (1) actually produces the wave number η as a function of the absorption coefficient a_η rather than the other way around. Thus, in dimensionless terms, it gives the function

$$\eta^* = \eta^*(a^*_\eta, \beta). \tag{3}$$

When required, the inverse function of that in Eq. (3), that is the function in Eq. (2), can be found by a numerical inversion technique (based on root-finding). However, the inversion process can be computationally demanding if the function $a^*_\eta = a^*_\eta(\eta^*, \beta)$ needs to be evaluated many times and, therefore, it is preferable to have the function in Eq. (2) when one wishes to produce a^*_η as a function of η^*.

Two representations of $\eta^*(a^*_\eta, \beta)$ and/or its inverse, $a^*_\eta(\eta^*, \beta)$ have been presented in the literature. Lee et al. [1] gave a fitted formula for $a^*_\eta(\eta^*, \beta)$, based on using Morizumi's expression for $A_l(s)$ [4], and Denison and Fiveland [3] gave a method for calculating $\eta^*(a^*_\eta, \beta)$, based on the expressions for $A_l(s)$ given by Edwards and Menard [5]. Lee et al. [1] had chosen Morizumi's expression to invert because it has continuous derivatives, whereas the Edwards and Menard relations are piecewise in nature. On the other hand, there is an uncertainty associated with evaluating parameters α and ω for the Morizumi model; as explained by Lee et al. [1], they are slightly path-length-dependent and deciding appropriate values requires some judgment. No such difficulties arise in the evaluation of the parameters in the case of the Edwards and Menard model used by Denison and Fiveland. Thus, the Denison and Fiveland model for the reordered band appears to be the preferred model, except for the fact that the model presents the formula in the form $\eta^*(a^*_\eta, \beta)$ rather than its inverse, $a^*_\eta(\eta^*, \beta)$. While this is not always a problem if one is using the smooth reordered distribution as an adjunct to the k-distribution method or the weighted sum of gray gases method, it *is* a problem if one is using it for the method of direct integration over wave number. So a direct formula for $a^*_\eta(\eta^*, \beta)$, like the one provided by Lee et al. [1] but founded on the Edwards and Menard [5] model for $A_l(s)$, is highly desired. Such an explicit formula is the subject of the present paper.

Before describing this new model, it is useful to provide additional motivation for its need. It will be recalled that the reordered band is useful for the k-distribution method and the weighted sum of gray gases method [3], as well as for the method where one integrates directly over wave numbers [1]. In the last of these methods, the direct form $a^*_\eta(\eta^*, \beta)$ is certainly the preferred one. In the weighted sum of gray gases method, it is true that one *can* proceed with the indirect form $\eta^*(a^*_\eta, \beta)$ and not need the direct form $a^*_\eta(\eta^*, \beta)$, and this was done in certain single component gas examples worked by Denison and Fiveland [3]. On the other hand, if there is soot present or there is more than one gaseous component so that there is a real possibility of overlapping bands, it will be necessary to add the contributions to the absorption coefficients at specific wave numbers, and this demands that one have the direct form $a^*_\eta(\eta^*, \beta)$ in order that one can add these contributions, if one is going to avoid the numerical inversion process. Thus the direct form may be useful in calculations using the weighted sum of gray gases method as well.

3. The new direct model, $a^*_\eta(\eta^*, \beta)$

Following a procedure similar to that of Lee et al. [1], a set of curves of the form $a^*_\eta(\eta^*, \beta)$ has been fitted to the smooth distribution of Denison and Fiveland [3], and interpolation between the curves is carried out using a cubic spline. Valid for the range $\beta \geqslant 0.003163$, the final formula for $a^*_\eta(\eta^*, \beta)$ is as follows:

$$a^*_\eta(\eta^*, \beta) = \sum_{k=1}^{11} \tilde{a}^*_\eta(\eta^*, k) \sum_{p=0}^{1} (-1)^p \Big[(B-p)\delta_{m+p,k} + B(B-1)(B+1-3p)\frac{c_{m+p,k}}{96} \Big], \tag{4}$$

where with

$$\chi = \chi(\beta) = \min(\beta, 1), \tag{5}$$

$$m = m(\beta) = 10 + \mathrm{int}(4\log_{10}\chi) \tag{6}$$

and

$$B = B(\beta) = \mathrm{int}(4\log_{10}\chi) - 4\log_{10}\chi, \tag{7}$$

and, with

$$\theta = \theta(\eta^*) = \max(\min\lfloor \ln(\eta^*), 2.5 \rfloor, -13.5), \tag{8}$$

Table 1
Coefficients, $b_{i,j}$, for the fitted smooth absorption coefficient distribution of Eq. (9)

$b_{i,j}$	$j=1$ (−2.5)	$j=2$ (−2.25)	$j=3$ (−2.0)	$j=4$ (−1.75)	$j=5$ (−1.5)	$j=6$ (−1.25)	$j=7$ (−1.0)	$j=8$ (−0.75)	$j=9$ (−0.5)	$j=10$ (−0.25)	$j=11$ (0.0)
$i=0$	−5.0919	−4.5484	−4.0255	−3.4832	−2.9781	−2.309	−1.8145	−1.3791	−1.1415	−1.1464	−1.1503
$i=1$	−2.2417	−2.2833	−2.4583	−2.9381	−2.8575	−2.351	−1.8516	−0.50116	−0.40397	−0.3352	−0.3239
$i=2$	−0.58104	−0.70131	−0.92055	−1.4214	−1.4243	−0.97896	−0.49942	0.066817	0.039895	0.05803	0.063837
$i=3$	−0.15008	−0.20101	−0.29246	−0.46655	−0.45399	−0.25242	−0.05054	−0.17001	−0.02017	−0.00229	0.000441
$i=4$	0	0	−0.00721	−0.02739	−0.02283	−0.00423	0	−0.02543	−0.00615	−0.00542	−0.0053
$i=5$	0	0	0	0	0	0	0	−0.00092	−0.00039	−0.00054	−0.00056
$i=6$	0.11709	0.15433	0.2336	0.43167	0.44625	0.29191	0.1021	−0.59715	−0.46281	−0.40421	−0.39649
$i=7$	0.002636	0.022312	0.057823	0.11905	0.12305	0.050379	−0.04822	0.20369	0.033764	−0.02117	−0.02937
$i=8$	−0.01961	−0.02678	−0.03625	−0.05013	−0.05566	−0.04316	−0.01079	−0.00635	0.012134	0.018849	0.019886
$i=9$	−8.5E−05	−6.5E−05	−0.00103	−0.00413	−0.00373	−0.00086	−3.6E−05	−0.00487	−0.0006	0.000813	0.00102
$i=10$	0	0	0	0	0	0	0	−0.00023	−0.00013	−0.00017	−0.00018

Corresponding values of $\log_{10}\beta$ given in brackets.

Table 2
Coefficients $c_{j,k}$ for Eq. (4)

$c_{j,k}$	$k=1$	$k=2$	$k=3$	$k=4$	$k=5$	$k=6$	$k=7$	$k=8$	$k=9$	$k=10$	$k=11$
$j=1$	0	0	0	0	0	0	0	0	0	0	0
$j=2$	26.2590	−59.5541	42.2165	−11.3119	3.0310	−0.8122	0.2176	−0.0583	0.0155	−0.0039	0.0006
$j=3$	−7.0361	42.2165	−70.8660	45.2475	−12.1240	3.2486	−0.8704	0.2332	−0.0622	0.0155	−0.0026
$j=4$	1.8853	−11.3119	45.2475	−71.6782	45.4651	−12.1823	3.2642	−0.8743	0.2332	−0.0583	0.0097
$j=5$	−0.5052	3.0310	−12.1240	45.4651	−71.7364	45.4807	−12.1862	3.2642	−0.8704	0.2176	−0.0363
$j=6$	0.1354	−0.8122	3.2486	−12.1823	45.4807	−71.7403	45.4807	−12.1823	3.2486	−0.8122	0.1354
$j=7$	−0.0363	0.2176	−0.8704	3.2642	−12.1862	45.4807	−71.7364	45.4651	−12.1240	3.0310	−0.5052
$j=8$	0.0097	−0.0583	0.2332	−0.8743	3.2642	−12.1823	45.4651	−71.6782	45.2475	−11.3119	1.8853
$j=9$	−0.0026	0.0155	−0.0622	0.2332	−0.8704	3.2486	−12.1240	45.2475	−70.8660	42.2165	−7.0361
$j=10$	0.0006	−0.0039	0.0155	−0.0583	0.2176	−0.8122	3.0310	−11.3119	42.2165	−59.5541	26.2590
$j=11$	0	0	0	0	0	0	0	0	0	0	0

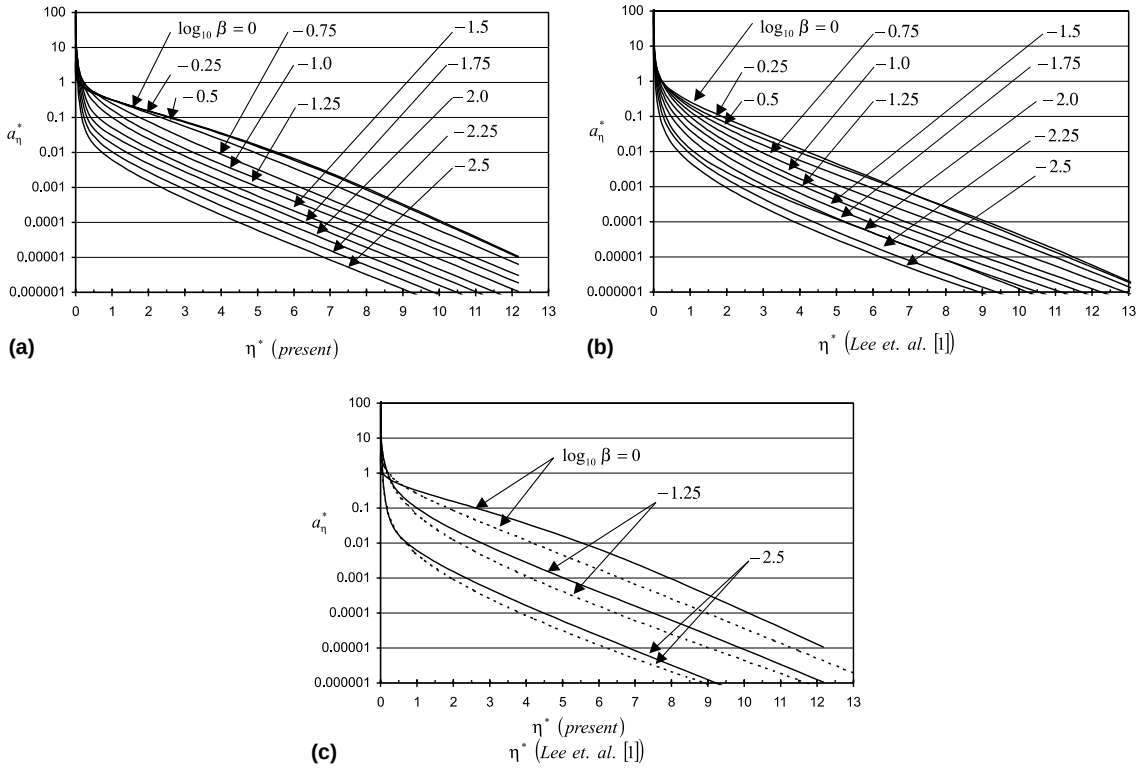

Fig. 1. The smooth absorption coefficient distribution according to: (a) the present work, (b) the work of Lee et al. [1] and (c) the present work (solid lines) and Lee et al. [1] (dashed lines).

$$\tilde{a}^*_\eta(\eta^*, j) = \exp\left\{\left(\sum_{i=0}^{5} b_{i,j}\theta^i\right)\left(1+\sum_{i=6}^{10} b_{i,j}\theta^{i-5}\right)^{-1}\right\}. \tag{9}$$

The coefficients $b_{i,j}$ in Eq. (9) are given in Table 1 and the coefficients $c_{j,k}$ of Eq. (4) are given in Table 2. The "int" function in Eqs. (6) and (7) returns the integral part of the argument; thus $\mathrm{int}(2.92) = 2$, and $\mathrm{int}(3.01) = 3$. The "min" function used in Eqs. (5) and (8) indicates that the minimum of the two arguments is to be taken: thus $\min(4.1, 5.2) = 4.1 = \min(5.2, 4.1)$. Similarly, the "max" function in Eq. (8) indicates that the maximum of the two arguments is to be taken: thus $\max(4.1, 5.2) = 5.2 = \max(5.2, 4.1)$. The function δ in Eq. (4) is the Kronecker delta. As a test on the correct usage of Eqs. (4)–(9), one can use the facts that
$a^*_\eta(3, 0.08) = 1.0785 \times 10^{-2}$,
$a^*_\eta(13.5, 0.08) = 1.5465 \times 10^{-6}$,
$a^*_\eta(8.3 \times 10^{-7}, 0.08) = 40.4713$ and
$a^*_\eta(3, 1.1) = 7.5603 \times 10^{-2}$.

The coefficients $b_{i,j}$ were obtained by using the Denison and Fiveland distribution to generate points (a^*_η, η^*) for the 11 specific values of $\log_{10}\beta$ running from -2.5 to 0.0 in steps of 0.25 (this corresponds to β running from 0.003163 to 1). For example, for $j = 5$, $\log_{10}\beta = -1.5$ as indicated in Table 1. For these specific values of β, $\tilde{a}^*_\eta(\eta^*, j)$ and $a^*_\eta(\eta^*, \beta)$ are identical functions of β and η^* . For each value of $\log_{10}\beta$, Eq. (9) was fitted to the points over a prescribed range in η^*, using a curve fitting computer software package, and the coefficients $b_{i,j}$ resulted from that fitting procedure. The "min" and "max" functions in Eq. (8) were used to ensure that the function in Eq. (9) does not go out of its fitted range. Once the function has been determined at these specific values of β, an interpolation can be used to find the function at intermediate values. Eq. (4) interpolates between the various β values, and the coefficients $c_{j,k}$ were determined by the 11-point cubic spline interpolation formula that was used, as were Eqs. (6) and (7).

Fig. 1 plots the smooth distribution of the present work, and the smooth distribution of Lee et al. [1] as well. (Note: the definition of η^* in the case of the Lee et al. distribution [1] is $\eta^* = |\eta - \eta_c|/\omega$ for a symmetric band, whereas $\eta^* = |\eta - \eta_c|/(\omega/2)$ in this paper.) The axes in Fig. 1 were constructed so that the distributions could be easily compared. As illustrated in Fig. 1(c), the smooth distribution of Lee et al. [1] predicts smaller

[1] The definition of η^* given in Lee et al. [1] was found to be in error.

Table 3
Values of $A^*(\tau)$ from the present work (RH), Denison and Fiveland [3] (DF), and Edwards and Menard [5] (EM)

Author	$\beta \setminus \tau$	0.001	0.01	0.1	1.0	10.0	100.0	1000.0
RH	0.01	9.99E − 04	9.03E − 03	5.33E − 02	1.89E − 01	6.39E − 01	1.96E + 00	4.01E + 00
	0.1	1.01E − 03	9.97E − 03	9.02E − 02	5.53E − 01	1.84E + 00	3.85E + 00	6.23E + 00
	1.0	1.01E − 03	1.00E − 02	9.83E − 02	8.19E − 01	3.33E + 00	6.12E + 00	8.48E + 00
DF	0.01	1.00E − 03	1.00E − 02	5.32E − 02	1.90E − 01	6.22E − 01	1.99E + 00	4.29E + 00
	0.1	1.00E − 03	1.00E − 02	1.00E − 01	5.32E − 01	1.90E + 00	4.20E + 00	6.51E + 00
	1.0	1.00E − 03	1.00E − 02	1.00E − 01	1.00E + 00	3.30E + 00	5.61E + 00	7.91E + 00
EM	0.01	9.98E − 04	9.01E − 03	5.31E − 02	1.91E − 01	6.32E − 01	1.96E + 00	4.06E + 00
	0.1	1.01E − 03	9.97E − 03	8.96E − 02	5.38E − 01	1.87E + 00	3.97E + 00	6.24E + 00
	1.0	1.01E − 03	1.01E − 02	9.88E − 02	8.24E − 01	3.34E + 00	6.05E + 00	8.41E + 00

absorption coefficients than the smooth distribution of the present work. This is consistent with the finding of Lee [6], who showed that the Morizumi expression [4] predicts smaller effective bandwidths than the Edwards and Menard expression [5], especially for large β. It should be noted, however, that since the bandwidth parameters, α and ω, are obtained differently according to the two methods, the comparison is more complicated than just comparing the two functions for a_η^*.

Values of $A^*(\tau) = A_l(s)/\omega$ were calculated over the range $0.01 \leqslant \beta \leqslant 1.0$ and $0.001 \leqslant \tau \leqslant 1000$ (where $\tau = \alpha\rho_a s/\omega$) using both the present smooth distribution and that of Denison and Fiveland [3]. Agreement with the A^* results from Denison and Fiveland was found to be within 3%, which is closer than the agreement between Denison and Fiveland [3] and the piece-wise function of Edwards and Menard [5]. Table 3 provides a comparison of the values of $A^*(\tau)$.

Carrying out calculations of total gas emissivity over a range of temperatures (500–2500 K) and a range of partial pressure path lengths (0.00305–0.914 atm m), for both H_2O and CO_2 gases verified the improvement in computational efficiency. It was found that, when performing the direct integration over wave number as illustrated in Eq. (10), use of the smooth distribution of the present work, $a_\eta^* = a_\eta^*(\eta^*, \beta)$, produced an approximately 100-fold reduction in calculation time as compared to numerically inverting the Denison and Fiveland function, $\eta^* = \eta^*(a_\eta^*, \beta)$, using the method of bisection.

4. Benchmark calculation of total gas emissivities

Benchmark comparisons for single, isothermal, homogeneous gases were carried out to check the accuracy of the new smooth absorption coefficient distribution, where the quantity used for comparison was the total gas emissivity. Total emissivity, $\varepsilon(L)$, of a gas, for path length L and temperature T_g, is defined as:

$$\varepsilon(L) \equiv \frac{1}{\sigma T_g^4} \int_0^\infty \left(1 - e^{-a_\eta L}\right) e_{b\eta}(T_g)\, d\eta, \tag{10}$$

where, now, we take into account all the relevant vibration–rotation bands. The quantity $e_{b\eta}(T_g)$ is the blackbody spectral emissive power of the gas at temperature T_g. Assuming a certain set of conditions, total emissivities of water vapour and of carbon dioxide, in a non-participating gas such as nitrogen, were generated by numerically integrating the smooth absorption coefficient distribution of the present work. The band parameters for CO_2 and H_2O were in accordance with those recommended by Edwards [7] and Modak [8].

The textbook by Modest [9] recommends the correlations of Leckner [10] for total gas emissivity. Leckner's charts are based on the integration of spectral data and show good agreement with other recent work. Fig. 2 compares total gas emissivities given by Leckner's correlations [10] with total gas emissivities generated from the smooth distribution of the present work. The concentration of the active gas is 0.305% by volume, the total pressure is 1.0 atm, and the path length is denoted by L. Although the band modeling work of Edwards and Menard [5], from which the smooth distribution was obtained, was independent of Leckner's correlations, the two methods produce total gas emissivities that agree reasonably well. Discrepancies tend to occur at higher temperatures where experimental data are more difficult to obtain.

5. Demonstration problem

The smooth absorption coefficient distribution can be applied to a wide variety of participating gas problems. For example, consider a spherical enclosure with gray and isothermal walls containing an isothermal and homogeneous gas. The gas is composed of a mixture of carbon dioxide and a non-participating carrier gas such as nitrogen. The following are the problem parameters:

Wall temperature: $T_w = 1000$ K.
Gas temperature: $T_g = 2000$ K.
Total pressure of the gas: $P_{total} = 1.0$ atm.
Partial pressure of CO_2 : $P_{CO_2} = 0.15$ atm.

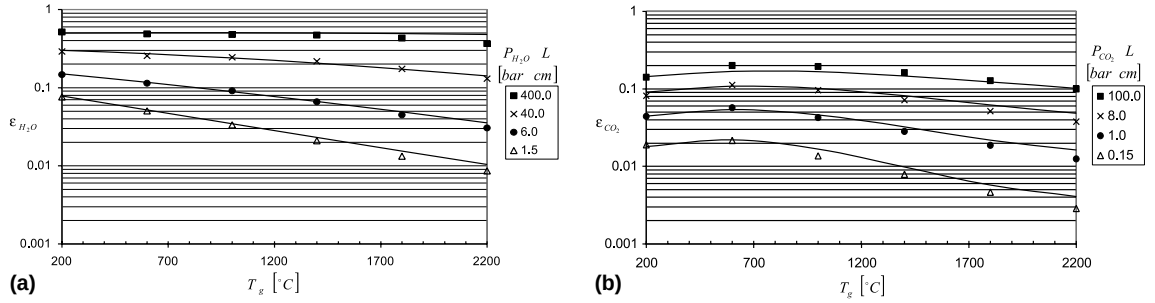

Fig. 2. Comparison of total gas emissivity predictions with those of Leckner for: (a) H_2O and (b) CO_2 in a non-participating gas. Solid lines: From the correlation of Leckner [10]. Symbols: From the smooth distribution of the present work.

The radius of the sphere, R, and the wall emissivity, ε_w, will vary. For the spherical enclosure with gray and isothermal walls containing an isothermal and homogeneous gas, there is an analytical solution for the net *spectral* radiant heat flux, $q_{w\eta}$, into the wall:

$$q_{w\eta} = \left[e_{b\eta}(T_w) - e_{b\eta}(T_g)\right]\left[\frac{\varepsilon_w(1-\overline{\tau}_\eta)}{1-(1-\varepsilon_w)\overline{\tau}_\eta}\right], \tag{11}$$

where

$$\overline{\tau}_\eta = \frac{1-(1+2a_\eta R)e^{-2a_\eta R}}{2(a_\eta R)^2}. \tag{12}$$

Integrating Eq. (11) over the thermal radiation spectrum provides q_w, the net *total* radiant heat flux into the wall. This integration can be carried out using the smooth absorption coefficient distribution.

The integration was performed numerically by dividing the thermal radiation spectrum (1–8000 cm^{-1}) into intervals within which the smooth absorption coefficient was assumed to be constant at its midpoint value. For the results plotted in Fig. 3(a), the radius, R, of the sphere is held constant at 5.0 m while the wall emissivity, ε_w, varies from 0.0 to 1.0. For Fig. 3(b), the wall emissivity is held constant at 0.8 while the radius varies from 0.01 to 100.0 m. Note that in Fig. 3(b), the net total radiant flux does not reach a horizontal asymptote when the radius becomes very large, as would be the case for a gray medium problem. This is to be expected for problems involving participating gases because the wings of the absorption bands become more important as the characteristic path length increases.

It should be noted that this solution of the spherical enclosure problem has been accomplished without making the mean beam length approximation, without making the band energy approximation [11], and without having to assume the black body radiation is constant over each band. It should also be noted that, once the band parameters (α, β, ω) had been calculated, the net total heat flux could be found using the integral function in the computer math software MATHCAD™. Calculation of the net total heat flux q_w required, on average, 5 s using MATHCAD™ on a personal computer.

6. Conclusions

A new smooth distribution of the form $a_\eta^* = a_\eta^*(\eta^*, \beta)$ has been fitted to the smooth distribution of Denison and Fiveland [3], which had been given in the form $\eta^* = \eta^*(a_\eta^*, \beta)$. The Denison and Fiveland [3] distribution had been derived from the Edwards and Menard

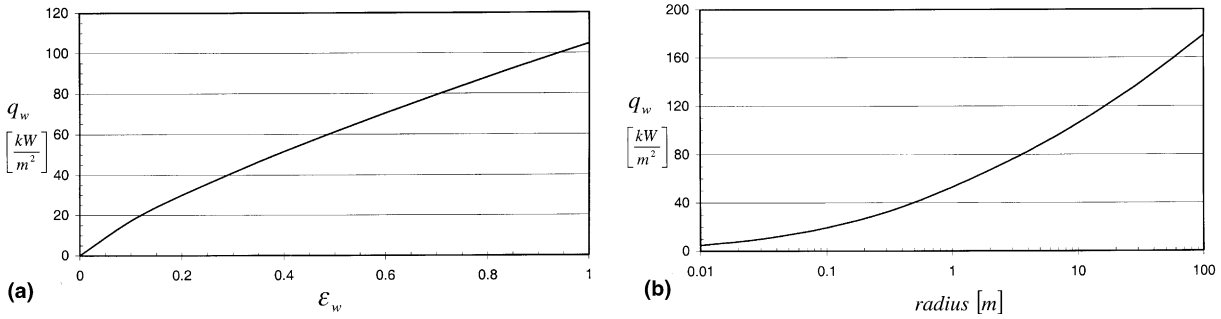

Fig. 3. The net total radiant heat flux into the wall versus: (a) wall emissivity (radius is 5.0 m); (b) radius (wall emissivity is 0.8).

[5] piecewise expression for effective bandwidth and, therefore, the correction on wide band parameters suggested by Lee et al. [1] is not required. For calculations in which one wishes to produce a_η^* as a function of η^*, the new smooth distribution allows an approximately 100-fold reduction in calculation time as compared to numerically inverting the Denison and Fiveland [3] distribution using the method of bisection. Such calculations are needed for direct integration over wave number. Moreover, if there is soot present or there is more than one active gaseous component so that there is a real possibility of overlapping bands, it will be necessary to add the contributions to the absorption coefficients at specific wave numbers, and this demands that one have the direct form $a_\eta^*(\eta^*, \beta)$ if one is going to avoid the numerical inversion process. The new curve fit did not result in a significant loss of accuracy from the Denison and Fiveland [3] distribution and it produced total gas emissivities in good agreement with the correlations of Leckner [10]. A demonstration problem involving a spherical enclosure with reflective walls illustrated the utility of the smooth absorption coefficient distribution, as well as the ease of calculation.

Acknowledgements

This work was supported by the Program of Energy Research and Development (PERD) of the Government of Canada and by an Ontario Graduate Scholarship awarded to one of the authors (A.R.).

References

[1] P.Y.C. Lee, K.G.T. Hollands, G.D. Raithby, Reordering the absorption coefficient within the wide band for predicting gaseous radiant exchange, ASME J. Heat Transfer 118 (1996) 394–400.
[2] G. Pathasarathy, J.C. Chai, S.V. Patankar, A simple approach to non-gray gas modeling, Numer. Heat Transfer Part B (29) (1996) 113–123.
[3] M.K. Denison, W.A. Fiveland, A correlation for the reordered wave number of the wide-band absorptance of radiating gases, ASME J. Heat Transfer 119 (1997) 853–856.
[4] S.J. Morizumi, An investigation of infrared radiation by vibration–rotation bands of molecular gases, Ph.D. Thesis, University of California, Los Angeles, 1970.
[5] D.K. Edwards, W.A. Menard, Comparison of models for correlation of total band absorption, Appl. Opt. 3 (5) (1964) 621–625.
[6] P.Y.C. Lee, Reordering the absorption coefficient within the wide band for predicting gaseous radiant exchange, Ph.D. Thesis, Department of Mechanical Engineering, University of Waterloo, Waterloo, Canada, 1996.
[7] D.K. Edwards, in: Radiation Heat Transfer Notes, Hemisphere, New York, 1981, pp. 195–239 (Chapter 5).
[8] A.T. Modak, Exponential wide band parameters for the pure rotational band of water vapour, J. Quant. Spectrosc. Radiat. Transfer 21 (1979) 131–142.
[9] M.F. Modest, in: Radiat. Heat Transfer, McGraw-Hill, New York, 1992, pp. 295–382 (Chapters 8 and 9).
[10] B. Leckner, Spectral and total emissivity of water vapor and carbon dioxide, Combust. Flame 19 (1972) 33–48.
[11] R. Siegel, J.R. Howell, in: Thermal Radiation Heat Transfer, third ed., Hemisphere, New York, 1992, pp. 607–609, ch. 13.